Journal of Nonlinear and Convex Analysis
Volume 26, Number 7, 2025, 1987–1997

Yokohama Publishers
ISSN 1880-5221 ONLINE JOURNAL

OSPREY MARINE PREDATOR ALGORITHM: AN ECONOMICAL OPTIMIZER FOR EQUITABLE POWER ALLOCATION IN NOMA-VLC SYSTEM

YUNSHAN SUN, GUANGZHAO WANG, JINGYU ZHANG, TING LIU*, YANQIN LI, AND TENG FEI

Abstract. This paper addresses the limitations of Marine Predator Algorithm (MPA), notably its slow convergence rate and tendency to become trapped in local optima when applied to complex optimization problems. This introduces Osprey Marine Predator Algorithm (OMPA) as an enhanced algorithm integrating strategic elements from many algorithms to improve MPA's performance. Benchmark test function experiments show that OMPA algorithm not only outpaces original MPA and its refined variants in convergence rate and precision but also outperforms various other reputable Metaheuristic Algorithms (MAs). These findings highlight OMPA's superior performance in addressing complex optimization problems. Furthermore, applying OMPA in an indoor Visible Light Communication (VLC) system employing Non-Orthogonal Multiple Access (NOMA) seeks to enhance power allocation among multiple users, maximizing overall sum rate while meeting stringent power allocation and Quality of Service requirements. Simulation studies demonstrate that OMPA achieves significant advantages in Log Sum Rate and Min Rate under various conditions, including challenging environments and diverse user configurations, and exhibits a notably faster convergence speed in multi-user scenarios than other algorithms.

1. Introduction

With the deployment of 5G networks, traditional Orthogonal Multiple Access (OMA) fails to handle the increasing user density and network traffic. Thus, NOMA has been identified as a promising solution for B5G, facilitating improved spectral efficiency and greater user concurrency by leveraging power-domain multiuser access. VLC utilizes the visible light spectrum for data transmission. To improve system utilization and power efficiency, researchers have integrated NOMA and VLC as effective solutions for B5G networks [14]. As issues become more complex, traditional deterministic algorithms encounter performance limitations [2]. In contrast, MAs stochastically explore the solution space, effectively avoiding local optima and making them suitable for complex constrained problems across various fields. MAs typically involve two phases: Exploration and Exploitation [20]. The 'No Free Lunch'(NFL) [22] asserts that no single optimization algorithm excels in all

---

2020 *Mathematics Subject Classification.* 68T20, 94-10.

Key words and phrases. Marine predator algorithm, osprey optimization algorithm, non-orthogonal multiple access, visible light communication.

This study was supported by Tianjin Science and Technology Plan Project Title: Research on Multidimensional Optimization Methods for Intelligent AI Manufacturing Technology in Complex Scenarios Project No. 24YDTPJC00600.

*Corresponding author.

domains, necessitating the consideration of specific problem characteristics when selecting or designing an algorithm, which explains the diversity in the metaheuristics field. Inspired by marine predators' foraging behavior, Marine Predator Algorithm (MPA) [8]. Performance improvements have been achieved through the development of hybrid algorithms that combine MPA with additional MAs. For example, Ghoneimy et al. [11] proposed the Differential Evolution Marine Predator (DEMP) algorithm, integrating Binary Differential Evolution (BDE) with MPA for better clustering accuracy, while Salgotra et al. [19] proposed a hybrid model of MPA and naked mole-rat algorithm (NMRA) to integrate the strengths inherent in each algorithm. MAs are crucial for optimizing power allocation in 5G networks. Pham et al. [17] applied Harris Hawks Optimization (HHO) algorithm with artificial neural networks for UAV positioning and power distribution in NOMA-VLC systems. Ali Safaa Sadiq et al. [18] introduced Nonlinear Marine Predator Algorithm (NMPA) to optimize power allocation and user fairness in NOMA-VLC networks. Gao et al. [10] developed the Quantum Carnivorous Plant Algorithm (QCPA) to optimize power allocations in NOMA systems, enhancing overall performance. Additionally, Sohail et al. [21] integrated user pairing, antenna height, and power allocation using Cat Swarm Optimization (CSO) to achieve higher gains and lower power consumption, while Hao et al. [12] employed Black Widow Enhanced Kepler Optimization Algorithm to maximize sum rates under Quality of Service (QoS) constraints.

Despite advancements in NOMA-VLC power allocation, challenges remain, particularly with limited generalization and the inability to guarantee the Min Rate. This study proposes a hybrid optimization method that combines multiple MAs to enhance adaptability and performance. Compared to existing methods, it enhances both the Log Sum Rate and Min Rate, thereby advancing NOMA-VLC applications in the B5G era.

2. Marine predator algorithm

MPA search through three phases: initialization, prey updating, and FADs' effect.

2.1. Initialization.

MPA generates the initial prey population through the equation: $x_{i,j} = x_{\min} + \text{rand}(x_{\max} - x_{\min}), \quad i = 1, 2, \ldots, N, \quad j = 1, 2, \ldots, D.$

In MPA, oceanic organisms are categorized into two groups: $\overrightarrow{\text{Elite}}$ and $\overrightarrow{\text{Prey}}$. This requires defining two $N \times D$ matrices, one for $\overrightarrow{\text{Prey}}$, as shown in equations (2.1), and another for $\overrightarrow{\text{Elite}}$, presented in equation (2.2).

$$\overrightarrow{\text{Prey}} = \left[\overrightarrow{\text{Prey}_1} \quad \ldots \quad \overrightarrow{\text{Prey}_i} \quad \ldots \quad \overrightarrow{\text{Prey}_N}\right]^\top, \tag{2.1}$$

$$\overrightarrow{\text{Elite}} = \left[\overrightarrow{\text{Elite}_1} \quad \ldots \quad \overrightarrow{\text{Elite}_i} \quad \ldots \quad \overrightarrow{\text{Elite}_N}\right]^\top. \tag{2.2}$$

2.2. Prey updating.

2.2.1. *Exploration phase.* During the exploration phase $t < \frac{T}{3}$, the algorithm focuses on exploring the search space.

$$\begin{cases} \overrightarrow{\text{stepsize}_i} = \overrightarrow{\text{R}_B} \otimes \left(\overrightarrow{\text{Elite}_i} - \overrightarrow{\text{R}_B} \otimes \overrightarrow{\text{Prey}_i}\right), \\ \overrightarrow{\text{Prey}_i} = \overrightarrow{\text{Prey}_i} + P \cdot \overrightarrow{\text{R}_1} \otimes \overrightarrow{\text{stepsize}_i}, \end{cases} \quad i = 1, 2, \ldots, N. \tag{2.3}$$

Where $\overrightarrow{\text{stepsize}_i}$ denotes the moving step vector and $\overrightarrow{\text{R}_B}$ is a vector of normally distributed random values used to represent Brownian motion, and we hold the scalar P constant at 0.5.The symbol $\otimes$ represents entry-wise multiplication. $\overrightarrow{\text{R}_1}$ denotes a uniformly distributed random vector between $[0, 1]$.

2.2.2. *Transition between exploration and exploitation.* When$\frac{T}{3} < t < \frac{2}{3}T$, the algorithm is in the transition phase between exploration and exploitation, as shown in equations (2.4) to (2.6):

$$\begin{cases} \overrightarrow{\text{stepsize}_i} = \overrightarrow{\text{R}_L} \otimes \left(\overrightarrow{\text{Elite}_i} - \overrightarrow{\text{R}_L} \otimes \overrightarrow{\text{Prey}_i}\right), \\ \overrightarrow{\text{Prey}_i} = \overrightarrow{\text{Prey}_i} + P \cdot \overrightarrow{\text{R}_1} \otimes \overrightarrow{\text{stepsize}_i}, \end{cases} \quad i = 1, 2, \ldots, \frac{N}{2}, \tag{2.4}$$

$$\begin{cases} \overrightarrow{\text{stepsize}_i} = \overrightarrow{\text{R}_L} \otimes \left(\overrightarrow{\text{R}_B} \otimes \overrightarrow{\text{Elite}_i} - \overrightarrow{\text{Prey}_i}\right), \\ \overrightarrow{\text{Prey}_i} = \overrightarrow{\text{Prey}_i} + P \times CF \otimes \overrightarrow{\text{stepsize}_i}, \end{cases} \quad i = \frac{N}{2} + 1, \ldots, N, \tag{2.5}$$

$$CF = \left(1 - \frac{t}{T}\right)^{2 \cdot \frac{t}{T}}. \tag{2.6}$$

Where: CF is a parameter control factor. $\overrightarrow{\text{R}_L}$ represents the random vector generated by the Lévy distribution.

2.2.3. *Exploitation phase.* When the $t > \frac{2}{3}T$predator uses Lévy distribution for exploitation. Its mathematical model is shown in equation (2.7):

$$\begin{cases} \overrightarrow{\text{stepsize}_i} = \overrightarrow{\text{R}_L} \otimes \left(\overrightarrow{\text{R}_L} \otimes \overrightarrow{\text{Elite}_i} - \overrightarrow{\text{Prey}_i}\right), \\ \overrightarrow{\text{Prey}_i} = \overrightarrow{\text{Elite}_i} + P \times CF \otimes \overrightarrow{\text{stepsize}_i}, \end{cases} \quad i = 1, \ldots, N. \tag{2.7}$$

2.3. **Eddy formation and FADs' effect.** Marine predators are influenced by environmental factors, including eddies and Fish Aggregating Devices (FADs). In MPA, are identified as potential points where the algorithm might become confined to local optima [8], and longer jumps are viewed as a way to avoid local optimal stagnation.

$$\overrightarrow{\text{Prey}_i} = \begin{cases} \overrightarrow{\text{Prey}_i} + CF\left[\overrightarrow{\text{x}_{\min}} + \overrightarrow{\text{R}_1} \otimes (\overrightarrow{\text{x}_{\max}} - \overrightarrow{\text{x}_{\min}})\right] \otimes \overrightarrow{\text{U}}, & \text{if } r_1 \leq FADs, \\ \overrightarrow{\text{Prey}_i} + [FADs\,(1 - r_1) + r_1]\left(\overrightarrow{\text{Prey}_{r1}} - \overrightarrow{\text{Prey}_{r2}}\right), & \text{if } r_1 > FADs. \end{cases} \tag{2.8}$$

Where $FADs$ represents the probability affecting the optimization process, with a value of 0.2; The binary vector $\overrightarrow{\text{U}}$ consists of elements 0 and 1, and r_1 represents a random value drawn uniformly between $[0, 1]$.

3. Osprey marine predator algorithm

3.1. **The position identification strategy of OOA.** In MPA, the $\overrightarrow{\text{Elite}}$ consists solely of optimal individuals, leading to underutilization of the broader population information. To enhance information exchange between populations and overcome these limitations, we have incorporated the position identification strategy from Osprey Optimization Algorithm (OOA) [7].

$$\overrightarrow{\text{F}} = \begin{bmatrix} F_1 & \dots & F_i & \dots & F_N \end{bmatrix}^\top = \begin{bmatrix} F(\overrightarrow{\text{Prey}_1}) & \dots & F(\overrightarrow{\text{Prey}_i}) & \dots & F(\overrightarrow{\text{Prey}_N}) \end{bmatrix}^\top . \tag{3.1}$$

In this context, assuming the problem is a minimization problem, an element is randomly selected from the $\{j \mid F_j < F_i,\ 1 \le j \le N,\ j \ne i\}$ and denoted as k_i, $k_i \in \{j \mid F_j < F_i,\ 1 \le j \le N,\ j \ne i\}$. $\overrightarrow{\text{F}}$ denotes a vector of fitness values. Then, the new i-th predator can be represented $\overrightarrow{\text{FP}_i}$ as:

$$\overrightarrow{\text{FP}_i} = \begin{cases} \overrightarrow{\text{Prey}_{k_i}}, & \text{if } r_2 \ge 0.5, \\ \overrightarrow{\text{Elite}_i}, & \text{otherwise.} \end{cases} \tag{3.2}$$

Where, r_2 represents a random value drawn uniformly between $[0, 1]$.This approach replaces the single $\overrightarrow{\text{Elite}_i}$ population in MPA with a suitable predator for each prey i. Any individual with a higher fitness value than the current prey can be considered a potential predator. In this model, we replace $\overrightarrow{\text{Elite}_i}$ in the equations. (2.3), (2.4), (2.5), and (2.7) with $\overrightarrow{\text{FP}_i}$:

$$\overrightarrow{\text{stepsize}_i} = \overrightarrow{\text{R}_B} \otimes \left(\overrightarrow{\text{FP}_i} - \overrightarrow{\text{R}_B} \otimes \overrightarrow{\text{Prey}_i} \right), \quad i = 1, 2, \dots, N, \tag{3.3}$$

$$\overrightarrow{\text{stepsize}_i} = \overrightarrow{\text{R}_L} \otimes \left(\overrightarrow{\text{FP}_i} - \overrightarrow{\text{R}_L} \otimes \overrightarrow{\text{Prey}_i} \right), \quad i = 1, 2, \dots, \frac{N}{2}, \tag{3.4}$$

$$\overrightarrow{\text{stepsize}_i} = \overrightarrow{\text{R}_L} \otimes \left(\overrightarrow{\text{R}_B} \otimes \overrightarrow{\text{FP}_i} - \overrightarrow{\text{Prey}_i} \right), \quad i = \frac{N}{2} + 1, \dots, N, \tag{3.5}$$

$$\overrightarrow{\text{stepsize}_i} = \overrightarrow{\text{R}_L} \otimes \left(\overrightarrow{\text{R}_L} \otimes \overrightarrow{\text{FP}_i} - \overrightarrow{\text{Prey}_i} \right), \quad i = 1, 2, \dots, N. \tag{3.6}$$

3.2. **Nonlinear parameter control strategy.** Nonlinear parameter control strategy CF effectively balances exploration and exploitation [16]. Its adoption enhances the algorithm's ability to explore high-dimensional search spaces, significantly improving optimization efficiency and search quality [9].

$$CF_{\text{New}} = 1 - \sin\left(\frac{\pi}{2} \times \left(\frac{t}{T} \right)^2 \right). \tag{3.7}$$

3.3. **The mutation strategy of OOBO.** In the simulated marine ecosystem, some less adapted prey enhance their survival chances through mutation, making it difficult for more adapted predators to capture them.Based on this biological principle, the mutation strategy in One-to-One-Based Optimizer (OOBO) [5] is introduced, and the algorithm further incorporates a stochastic yet controlled mutation mechanism.

$$\overrightarrow{\text{Prey}_i^{\text{new}}} = \overrightarrow{\text{Prey}_i} + \overrightarrow{\text{R}_2} \otimes \left(\overrightarrow{\text{FP}_i} - I \otimes \overrightarrow{\text{Prey}_i} \right), \tag{3.8}$$

$$I = \text{round}(1 + r_3). \tag{3.9}$$

Where, $\overrightarrow{\text{R}_2}$ denotes a uniformly distributed random vector between $[0,1]$, I is a random factor, with round being the rounded value of I, adjusted to either 1 or 2 to aid decision-making or incorporate randomness into the calculations and r_3 represents a random value drawn uniformly between $[0,1]$.

$$\overrightarrow{\text{Prey}_i} = \begin{cases} \overrightarrow{\text{Prey}_i^{\text{new}}}, & \text{if } F_i^{\text{new}} < F_i, \\ \overrightarrow{\text{Prey}_i}, & \text{else.} \end{cases} \tag{3.10}$$

The diagrammatic representation of the Flowchart of OMPA algorithm is placed by Figure 1.

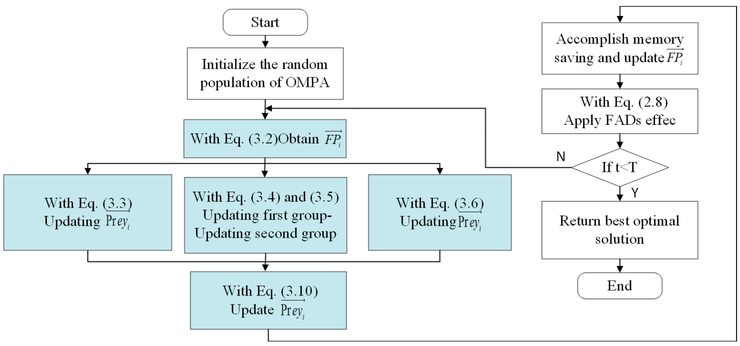

Figure 1. Flowchart of OMPA algorithm.

3.4. **Computational complexity.** Complexity analysis is crucial for evaluating an algorithm's efficiency, focusing on repeated operations. The time complexity (TC) of MPA is determined by N, D, and T. Specifically, initializing the population takes $O(N \times D)$, marine memory updating $O(N \times T)$, elite population selection $O(N \times T)$, and prey position updating $O(N \times D \times T)$. Thus, the overall time complexity of MPA is $O(N \times D \times T)$. Although OMPA introduces additional steps like elite population selection and marine memory management, the overall time complexity remains the same.

4. Results and discussions

To evaluate OMPA's performance, this study uses the CEC2022 benchmark [4], comparing it with Particle Swarm Optimization (PSO) [15], Whale Optimization Algorithm (WOA) [23], Dung Beetle Optimizer (DBO) [18], Coati Optimization Algorithm (COA) [5], Young's Double-Slit Experiment optimizer (YDSE) [1] and NMPA [18]. The results demonstrate OMPA's superior optimization performance across multiple scenarios. Figure 2 illustrates OMPA's enhanced accuracy and faster convergence. All algorithm parameters are set according to the specifications outlined in their respective studies and are summarized in Table 1. Table 2 presents the

Wilcoxon rank-sum statistical test at $\alpha = 0.05$, confirming that OMPA outperforms the original MPA on CEC2022.

TABLE 1. Algorithms' parameter values

Algorithm	Year	Parameters Values
PSO	1995	$w_{\text{Max}} = 0.9$, $w_{\text{Min}} = 0.2$, $c_1 = 2$, $c_2 = 2$
WOA	2016	The value of a linearly decreases from 2 to 0.
DBO	2022	$P_{\text{percent}} = 0.2$
COA	2023	—
YDSE	2023	$L = 1$, $d = 5 \times 10^{-3}$, $I = 0.01$, $\Lambda = 5 \times 10^{-6}$, $\Delta = 0.38$
MPA	2020	FADs $= 0.2$, $P = 0.5$
NMPA	2022	FADs $= 0.2$, $P = 0.5$

TABLE 2. Wilcoxon rank sum test p values of MPA

No.	F1	F2	F3	F4	F5	F6
MPA	1.1E-07	8.0E-01	3.4E-07	6.8E-01	6.9E-04	1.0E-03
$+/=/-$	$-$	$=$	$-$	$=$	$-$	$-$
No.	F7	F8	F9	F10	F11	F12
MPA	3.6E-03	4.2E-05	5.2E-07	3.6E-02	1.8E-05	7.1E-01
$+/=/-$	$-$	$-$	$-$	$-$	$-$	$=$

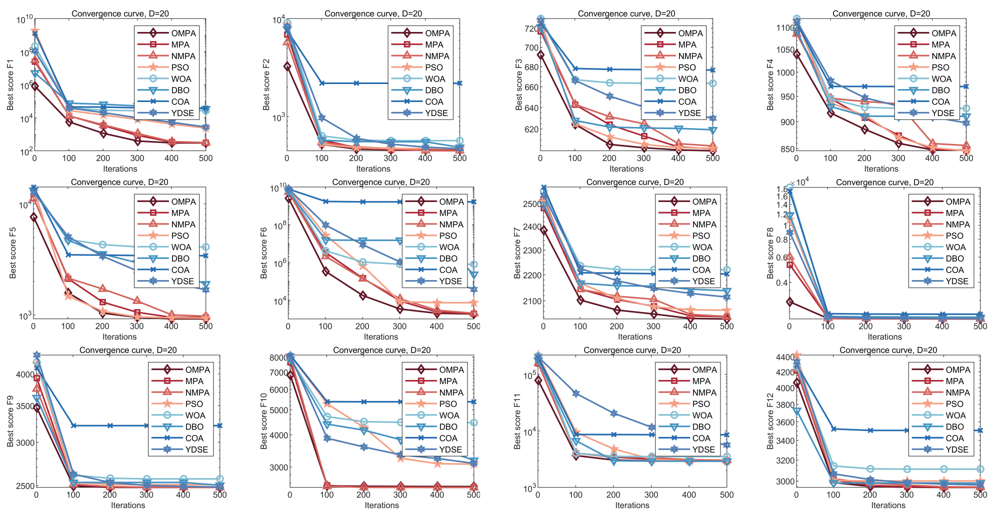

FIGURE 2. Convergence curves of OMPA and other MAs

5. FIELD APPLICATION: FAIR POWER DISTRIBUTION IN NOMA-VLC SYSTEMS

The illustration of a VLC network with NOMA is provided in Figure 3.

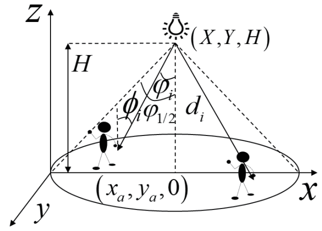

FIGURE 3. llustration of a VLC network with NOMA

We implement the Line-of-Sight (LoS) propagation path and adopt the generalized Lambertian emission model. The number of users is denoted by I, and the channel gain h_a for the a-th user ($a \in [1, I]$) is expressed in equation (5.1) as follows:

$$h_a = \frac{A_a}{d_a^2} R_o(\varphi_a) T_s(\phi_a) g(\phi_a) \cos(\phi_a). \tag{5.1}$$

Where, A_a are the detection area, d_a the distance between the user and LED transmitter, as given by $d_a = \sqrt{(X - x_a)^2 + (Y - y_a)^2 + H^2}$. φ_a and the angles of irradiance LED and incidence, respectively, $T_s(\phi_a)$ is the gain of the optical filter to be 1, $g(\phi_a) = \frac{n^2}{\sin(\phi_{FoV})}$ $0 \le \phi_a \le \phi_{FoV}$ denotes the concentrator gain,$R_0(\varphi_a) = \frac{m+1}{2\pi}\cos^m(\varphi_a)$ is the Lambertian radiant intensity, where $\cos(\varphi_a) = \cos(\phi_a) = \frac{H}{d_a}$. With, $n = 1.5$ being the internal refractive index, ϕ_{FoV} is the Field of View (FoV), $\varphi_{1/2}$ is transmitter semiangle at half power and $m = -\ln 2 / \ln(\cos(\varphi_{1/2}))$.

According to the reference [3], the data rate for NOMA downlink is as follows:

$$R_a = B \log_2 \left(1 + \frac{h_a p_a}{h_a \sum_{l=a+1}^{I} p_l + n_o} \right). \tag{5.2}$$

Where, p_a is the power obtained by the a-th user, B is the transmission bandwidth of each channel, and n_0 is defined as the noise power.

The power allocation optimization challenge within NOMA-VLC is defined by :

$$\begin{aligned} &P1 : \max R = \sum_{a=1}^{I} \log_2(R_a), \\ &\text{s.t.} \begin{cases} C_1 : p_a \ge 0, \ \forall\, I, & C_2 : \sum_{a=1}^{I} p_a \le p_{\max}, \\ C_3 : p_1 < p_2 < \cdots < p_I, \ \forall\, I, & C_4 : \sum_{a=1}^{I} \sqrt{p_a} \le \frac{\min\{D, C-D\}}{\delta}. \end{cases} \end{aligned} \tag{5.3}$$

Where, $p_{\max}$ is the maximal transmit power, D is the DC-offset ($D = 20$), C is the peak optimal density ($C = 30$), and $\delta = \frac{3\sqrt{5}}{5}$ is a coefficient by Pham et al. [17]. To conduct the tests, we must first establish several key system parameters which are $5m \times 5m \times 3m$, $A_a = 0.0001m^2$, $B = 10$MHz, and $n_0 = -104$dBm. OMPA is compared against several established MAs using two key metrics: 1. **Log Sum**

Rate, calculated by the objective function equation. (5.3) to maximize the system's rate performance by evaluating the Log Sum Rates of all users. 2. **Min Rate**, which indicates the lowest rate among all users. The inclusion of constraints reduces the solution space, potentially minimizing the performance disparity between OMPA and other algorithms.

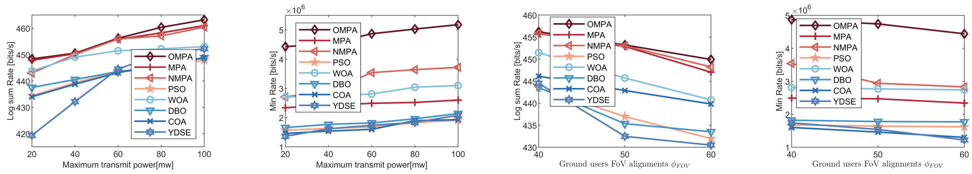

FIGURE 4. Log Sum Rate and Min Rate under different conditions

The first two plots of Figure 4 illustrate the effect of varying $p_{\max}$ on system performance. OMPA's Log Sum Rate outperforms MPA and other MAs due to its efficient power allocation, maximizing the Log Sum Rate while enhancing user fairness. The last two plots show the impact of different receivers ϕ_{FoV} on the system rate. As ϕ_{FoV} increases, both the Log Sum Rate and Min Rate gradually decrease. However, the OMPA maintains a high rate across various reception conditions, demonstrating its robustness and stability.

The experiment was set with $p_{\max} = 60$mW, $\phi_{FoV} = 40°$, and $\varphi_{1/2} = 45°$. Figure 5 presents the convergence plots. The first two plots related to the Log Sum Rate demonstrate that the OMPA algorithm converges more quickly as the number of users increases and achieves the highest Log Sum Rate. This indicates the algorithm's efficiency in finding optimal solutions. The last two plots focus on the Min Rate performance.As the user count reaches 30, other algorithms tend to fall into local optima, whereas OMPA consistently ensures the highest transmission rate for disadvantaged users, demonstrating its superior overall performance and fairness across varying user numbers.Table 3 presents Wilcoxon rank-sum statistical test results at $\alpha = 0.05$, confirming that OMPA outperforms MPA.

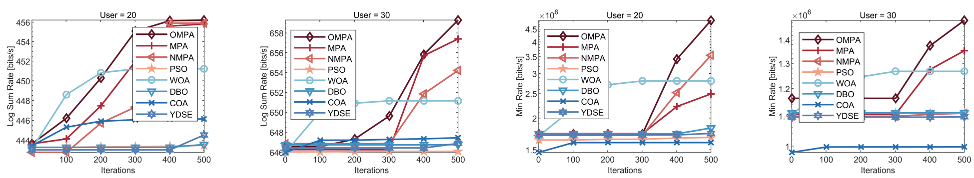

FIGURE 5. Log Sum Rate and Min Rate against the number of Users

Simulations demonstrate that, in the NOMA-VLC system, OMPA outperforms other algorithms in both Log Sum Rate and Min Rate, especially with an increasing number of users..Its rapid convergence makes it well-suited for dynamic networks by efficiently adapting to changes in users and conditions.While OMPA performs comparably to other algorithms at low user counts, it significantly outperforms them at higher user counts, positioning it as a robust tool for future network optimization.

Table 3. Wilcoxon rank sum test p-values of MPA

	Log Sum Rate		**Min Rate**	
User	20	30	20	30
MPA	2.2E-04	1.8E-04	1.1E-06	1.7E-04
$+/=/-$	$-$	$-$	$-$	$-$

6. Conclusion and future works

Introducing OMPA, an improved variant of MPA that overcomes challenges related to local optima and slow convergence. It achieves this by incorporating a nonlinear parameter control strategy, OOA for elite population diversification, and OOBO for adaptive mutations.These improvements result in faster convergence, increased accuracy, and the ability to escape local optima. Benchmarking against CEC2022 problems demonstrates OMPA's superior performance. Moreover, OMPA's application in optimizing power allocation and ensuring Min Rate in NOMA-VLC systems underscores its practical effectiveness. This validation reinforces OMPA's applicability in real-world scenarios and contributes to the advancement of algorithmic development. Future work will focus on exploring OMPA's application in diverse systems to further refine and adapt the algorithm.

References

[1] M. Abdel-Basset, D. El-Shahat, M. Jameel and M. Abouhawwash, *Young's double-slit experiment optimizer: a novel metaheuristic optimization algorithm for global and constraint optimization problems*, Computer Methods in Applied Mechanics and Engineering **403** (2023): 115652.

[2] B. Abdollahzadeh, F. Soleimanian Gharehchopogh and S. Mirjalili, *Artificial gorilla troops optimizer: a new nature-inspired metaheuristic algorithm for global optimization problems*, International Journal of Intelligent Systems **36** (2021), 5887–5958.

[3] M. S. Ali, H. Tabassum and E. Hossain, *Dynamic user clustering and power allocation for uplink and downlink non-orthogonal multiple access (noma) systems*, IEEE Access **4** (2016), 6325–6343.

[4] S. B. Aydemir, *Enhanced marine predator algorithm for global optimization and engineering design problems*, Advances in Engineering Software **184** (2023): 103517.

[5] M. Dehghani, Z. Montazeri, E. Trojovská and P. Trojovský, *Coati optimization algorithm: a new bio-inspired metaheuristic algorithm for solving optimization problems*, Knowledge-Based Systems **258** (2023): 110011.

[6] M. Dehghani, E. Trojovská, P. Trojovský and O. P. Malik, *OOBO: A new metaheuristic algorithm for solving optimization problems*, Biomimetics **8** (2023): 468.

[7] M. Dehghani and P. Trojovsẏ, *Osprey optimization algorithm: a new bio-inspired metaheuristic algorithm for solving engineering optimization problems*, Frontiers in Mechanical Engineering **8** (2023): 1126450.

[8] A. Faramarzi, M. Heidarinejad, S. Mirjalili and A. H. Gandomi, *Marine predators algorithm: a nature-inspired metaheuristic*, Expert Systems with Applications **152** (2020): 113377.

[9] S. Fu, H. Huang, C. Ma, J. Wei, Y. Li and Y. Fu, *Improved dwarf mongoose optimization algorithm using novel nonlinear control and exploration strategies*, Expert Systems with Applications **233** (2023): 120904.

[10] H. Gao, Y. Di, L. Guo and L. Zhao, *Joint subchannel power allocation for downlink noma systems based on quantum carnivorous plant algorithm*, Journal of King Saud University - Computer and Information Sciences **36** (2024): 102051.

[11] M. Ghoneimy, H. Hassan and E. Nabil, *A new hybrid clustering method of binary differential evolution and marine predators algorithm for multi-omics datasets*, IJIES **14** (2021), 421–431.

[12] L. Hao, P. Cao, C. Li and Z. Xin, *A novel sum-rate maximization scheme for noma-vlc systems via the black widow enhanced Kepler optimization algorithm*, Optics Communications **573** (2024): 130979.

[13] J. Kennedy and R. Eberhart, *Particle swarm optimization*, in: Proceedings of ICNN'95 - International Conference on Neural Networks, Perth, WA, Australia: IEEE, vol. 4, 1995, pp. 1942–1948.

[14] T. Kishi, H. Tanaka, Y. Umeda and O. Takyu, *A high-speed led driver that sweeps out the remaining carriers for visible light communications*, Journal of Lightwave Technology **32** (2014), 239–249.

[15] S. Mirjalili and A. Lewis, *The whale optimization algorithm*, Advances in Engineering Software **95** (2016), 51–67.

[16] F. B. Ozsoydan, *Artificial search agents with cognitive intelligence for binary optimization problems*, Computers & Industrial Engineering **136** (2019), 18–30.

[17] Q.-V. Pham, T. Huynh-The, M. Alazab, J. Zhao and W.-J. Hwang, *Sum-rate maximization for uav-assisted visible light communications using Nnma: swarm intelligence meets machine learning*, IEEE Internet of Things Journal **7** (2020), 10375–10387.

[18] A. S. Sadiq, A. A. Dehkordi, S. Mirjalili and Q.-V. Pham, *Nonlinear marine predator algorithm: a cost-effective optimizer for fair power allocation in NOMA-VLC-B5G networks*, Expert Systems with Applications **203** (2022): 117395.

[19] R. Salgotra, S. Singh, U. Singh, S. Mirjalili and A. H. Gandomi, *Marine predator inspired naked mole-rat algorithm for global optimization*, Expert Systems with Applications **212** (2023): 118822.

[20] M. P. Saka, O. Hasançebi and Z. W. Geem, *Metaheuristics in structural optimization and discussions on harmony search algorithm*, Swarm and Evolutionary Computation **28** (2016), 88–97.

[21] M. F. Sohail, C. Y. Leow and S. Won, *A cat swarm optimization based transmission power minimization for an aerial noma communication system*, Vehicular Communications **33** (2022): 100426.

[22] D. H. Wolpert and W. G. Macready, *No free lunch theorems for optimization*, IEEE Transactions on Evolutionary Computation **1** (1997), 67–82.

[23] J. Xue and B. Shen, *Dung beetle optimizer: a new meta-heuristic algorithm for global optimization*, J Supercomput **79** (2023), 7305–7336.

Manuscript received October 24, 2024
revised January 8, 2025

Y. S. SUN
College of Information Engineering, Tianjin University of Commerce, China
E-mail address: sunyunshan@tjcu.edu.cn

G. Z. Wang
College of Information Engineering, Tianjin University of Commerce, China
E-mail address: wangguangzhao@stumail.tjcu.edu.cn

J. Y. Zhang
China Mobile Communications Corporation, China
E-mail address: 13910029910@139.com

T. Liu
College of Information Engineering, Tianjin University of Commerce, China
E-mail address: liuting@tjcu.edu.cn

Y. Q. Li
College of Information Engineering, Tianjin University of Commerce, China
E-mail address: liyanqin-2190@126.com

T. Fei
College of Information Engineering, Tianjin University of Commerce, China
E-mail address: feiteng@tjcu.edu.cn